SRRC CONSTRUCTION AND COMMISSIONING RESULTS

Y.C. Liu[a)], J.R. Chen[b)] and C.C. Kuo
Synchrotron Radiation Research Center
No 1. R&D Rd VI, Hsinchu Science-Based Industrial Park, Hsinchu, Taiwan, R.O.C.
[a)]Department of Physics, National Tsing Hua University, Hsinchu, Taiwan, R.O.C.
[b)]also Institute of Nuclear Science, National Tsing Hua University, Hsinchu, Taiwan, R.O.C.

Abstract

A 1.3 GeV third generation synchrotron radiation facility has been constructed at the Synchrotron Radiation Research Center (SRRC) located in Hsinchu, Taiwan, Republic of China. At this moment, the storage ring is in the final commissioning stage. We had achieved a few mA stored beam in April 1993 in a very short period and some machine parameters had been measured. The theoretical and measured values were in good agreement.

I. INTRODUCTION

To provide bright, continuous and tunable VUV and soft x-ray light sources for researches ranging over the fields of physics, chemistry, biology, medicine, material science, etc., a dedicated third-generation synchrotron radiation facility was established in Taiwan. The SRRC accelerator complex, as shown in Fig. 1, consists of a 50 MeV e^- linac, a 1.3 GeV synchrotron booster [1,2], a 70 m long BTS transfer line [1,3], and a 1.3 GeV storage ring [1,4,5]. The injection system including linac and booster synchrotron was contracted out to Scanditronix AB, Sweden, and was officially turned over to SRRC in July 1992. It took about a year to install the BTS line and the storage ring, which started in March 1992 and was completed in March 1993. Beam tests in the BTS line started in August 1992 and were completed in January 1993. Up till now, the storage ring is in the final commissioning stage. The beam storage was accomplished in April 1993. We expect that the designed beam current of 200 mA will be achieved after the vacuum vessels have been baked out and cleaned by the synchrotron radiation. The schedule of the civil construction is briefly described in Sec. II. The design parameters and components are described in Sec. III. The installation activities are given in Sec. IV, and the early commissioning results are shown in Sec. V.

II CIVIL CONSTRUCTION

The SRRC civil construction can be divided into three phases. The Phase I construction including the Administration and Lab Building and the Machine shop was completed in May 1990. In June 1990, the entire staff moved into the site. The Phase II construction included the Booster and Storage Ring Buildings. By February 1991, the Booster

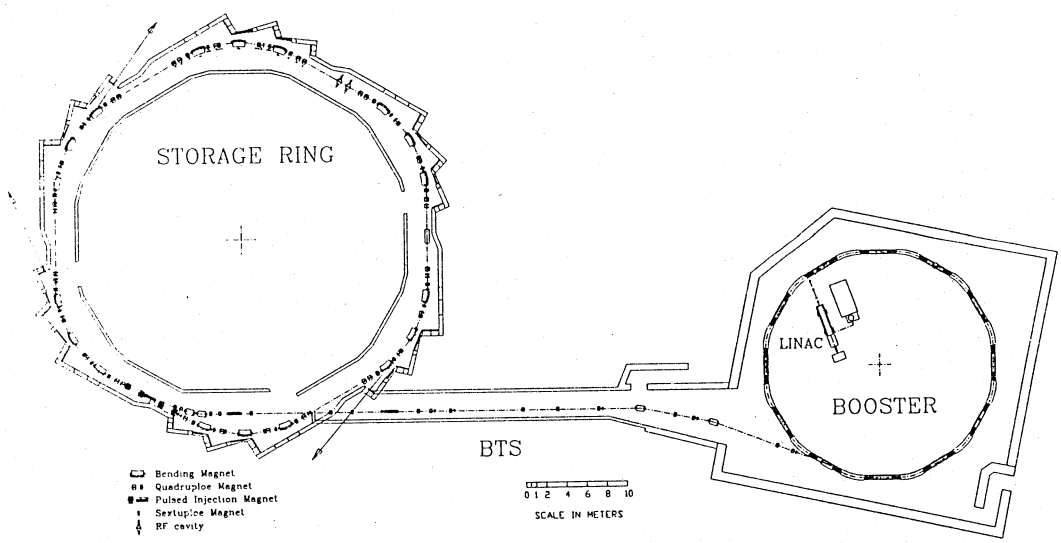

Fig.1 Layout of the SRRC accelerator complex: a 50 MeV linac, a 1.3 GeV booster and a 1.3 GeV storage ring.

Building was ready in time for the delivery of the injector components. In December 1991, the Storage Ring Building was completed. The beneficial occupancy of the civil construction was so smooth that no delay was caused in the installation and tests of the accelerator systems. The Phase III construction is the Guest House and will be ready in August 1993.

III DESIGN PARAMETERS AND COMPONENTS

A. injector

A 1.3 GeV full energy injection system was contracted out to Scanditronix AB, Sweden in August 1988. However, SRRC was fully responsible for the RF system of the booster synchrotron. Installation of the injector started in May 1991 and the beam tests began in January 1992. The performance and reliability of the injector were demonstrated before it was officially turned over to SRRC in July 1992. The major design parameters of the injector are listed in Table 1.

Table 1 Major Design Parameters of the Injector

Linac energy	50 MeV
Linac current	30 mA
(multibunch mode, averaged current)	
Linac RF frequency	2997.9 MHz
Booster energy	1.3 GeV
Booster circumference	72 m
Booster RF frequency	500 MHz
Booster natural emittance	$1.2\ 10^{-7}$ m-rad
Booster current (average)	
Multibunch mode	5 mA
Single bunch mode	0.3 mA
Booster repetition rate	10 Hz

The injector has been operating satisfactorily since it was taken over by SRRC. The machine parameters have been measured and are in agreement with the design values [2].

B. Storage Ring Lattice

The lattice structure is a combined-function triple-bend-achromat (TBA) type with 6-fold symmetry [1,4,5]. There are six dispersion free long straight sections, each 6 m, for the accommodation of the injection elements, RF cavities, undulators and wigglers. In Fig. 2, the lattice functions of one period of the ring are shown. The major parameters of the storage ring are listed in Table 2.

Table 2 Major Storage Ring Parameters

Energy	1.3 GeV
Circumference	120 m
Natural emittance	$1.92\ 10^{-8}$ m-rad
Nominal current, multibunch	200 mA
single bunch	5 mA
Natural energy spread, rms	$6.6\ 10^{-4}$
Tune ν_x/ν_y	7.18/4.13
Momentum compaction	0.00678
Radio frequency	500 MHz
RF cavity gap voltage (nominal)	800 kV
Synchrotron tune	$1.15\ 10^{-2}$
Number of dipole, quad, sext	18, 48, 24
Bending field	1.24 T
Damping time τ_x, τ_y, τ_s	10.691, 14.397, 8.708 ms
Critical photon energy in dipole	1.39 keV
Beam size at insertion middle	
Horizontal	0.45 mm
Vertical (10% emittance ratio)	0.024 mm

The dynamic aperture of the single particle dynamics and the collective effects of the particle beam were studied in detail. Fig. 3 depicts the dynamic aperture with and without the typical multipole errors for a 1000-turn single particle tracking which was obtained with the tracking code RACETRACK [6]. The acceptable tolerances of the magnetic properties and the alignment errors were given accordingly [1,3,4].

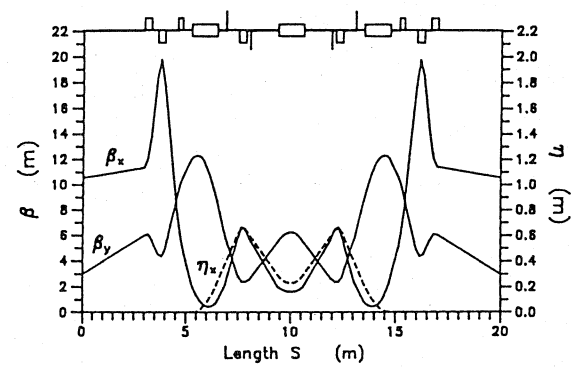

Fig. 2 The betatron and dispersion functions of one cell of the ring. The ring has six identical cells.

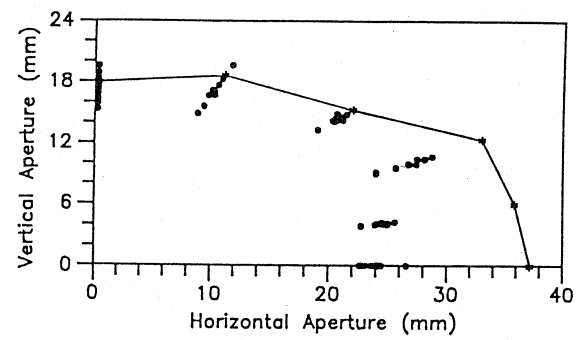

Fig. 3 The dynamic aperture of the storage ring with and without the typical multipole field errors.

C. Magnet and Power Supplies

There are 18 dipole magnets powered in series and four families of quadrupole magnets, each with 12 magnets powered in series. The chromaticities are corrected with 2 families of 24 sextupoles. In addition, there are 24 horizontal and 30 vertical correctors for orbit correction. Moreover, several skew quadrupoles were used for coupling correction. The magnets were designed, constructed, measured and analyzed in the site with care. All the magnets installed in the ring were within the acceptable tolerances in terms of the multipole errors and integrated fundamental field errors [1,7]. The pulsed magnets such as the septum and kickers also met the specifications.

D. Vacuum

Most of the vacuum chambers were made of aluminum. Much care was taken so as to provide an ultrahigh vacuum, low impedance environment. The cleanness of the material, the tapering of the chamber, the shielding of the bellows, the thermal load, the deformation, rigidity and flexibility of the supporting frame, etc., were seriously considered in order to meet the requirements. In the present, without turning on the ion pumps, the vacuum pressure is about 10^{-8} Torr without beam and about 10^{-7} Torr with a few mA stored beam current. The bakeout of the vacuum chamber has been carried out. After turning on the ion pumps, we expect that the vacuum pressure can reach 10^{-11} Torr without beam.

E. RF system

In one of the long straight sections, two Doris I type cavities purchased from DESY were installed. Each cavity is with 60 kW maximum RF power provided by individual transmitter purchased from the Mountain Technology, USA. The low level electronic control system was made in SLAC. The RF system of the booster is identical to the ones in the storage ring. The system can accelerate 1.3 GeV electron beam of more than 200 mA current in the presence of the insertion devices. The nominal RF frequency is 499.654 MHz. The RF systems, both in the booster and storage ring, have been operating with incredibly reliable performance.

F. Survey and Alignment

Extremely tight requirements on the alignment of the magnets, especially the quadrupole magnets of the ring in both transverse directions are necessary in order to reduce closed orbit distortions. The acceptable alignment errors in both planes are 0.15 mm rms and the rotation errors are 0.5 mrad rms. The quadrupole magnets were prealigned in the girders and then moved into the tunnel. The final results of the alignments for the dipoles and quadrupoles were 0.14 mm rms and 0.12 mm rms in the horizontal and vertical plane, respectively. The tilt errors were 0.2 mrad rms in the dipoles and 0.06 mrad rms in the quadrupoles. As for the sextupoles, the results were 0.20 mm rms and 0.15 mm rms in the horizontal and vertical plane respectively. All the alignment results were within acceptable tolerances. The measured closed orbit distortions were consistent with the simulated results and will be described in Sec. V.

G. Beam Diagnostics

There were seven screen monitors for the first turn beam observation in the ring. Among them, two were used for injection launching adjustments in the first commissioning stage. The number of the button type beam position monitors (BPM) was 47 in total. The processing electronic is shown in Fig. 4. The dynamic range of the BPM electronic was from 50 μA with resolution about 50μm to 200 mA with 10 μm resolution. Two linear tapered stripline electrodes were installed to measure the transverse motion and the bunch time structure. One excitation electrode station could be used for the tune measurements as well as for the transverse instability damping if needed. The fast beam signal, such as the filling structure, could also be measured using the fast current transformer and the precise beam current were obtained from the Bergoz's parametric current transformer (PCT) with resolution better than 1 μA. Some other elements such as the scraper, photon light monitor, etc., are described in Ref. [8].

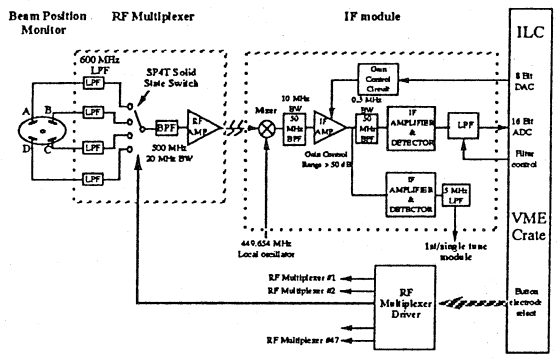

Fig. 4 The BPM processing electronic.

H. Control and Operation

The control hardware architecture adopted was a two level hierarchical system. Some VAX workstations running the VMS operating system were used for control computer system. Between the database and the subsystem devices, several intelligent local controllers (ILCs) were implemented. Both level computers, including the booster injector's, were linked via the Ethernet network. The control software system was divided into 4 layers. They were the device access, network access, database access, and the applications. A friendly graphical user interface (GUI)

operation panel was developed. It was very useful for the machine commissioning. The radiation safety interlock system was a self-protected subsystem and was also linked to the central control system [9].

IV. INSTALLATION

The installation task of such a rather complicated system indeed need well planning and full cooperation among all subsystems involved. A cell of 20 m long mocked-up was installed in the machine shop by end of 1991 and we gained a lot of practical experience. The installation of the BTS started in March 1992 and was completed in September 1992 except for the septum magnet. The installation of the ring began in March 1992. By May 1992, the cabling work and magnet stands installation were finished. The power supplies and all the magnets, except for the pulsed magnets, were installed by October 1992. Finally, the vacuum system including the diagnostics elements, RF cavities and the RF low level system were installed by end of 1993. In February 1993, we passed the full power test of the magnet power supplies and the ring chambers were connected as a closed form by then. Installation of the RF high power transmitter and the four kicker pulsers were finished in March 1993. The alignment of the magnets reached the acceptable level in March. In the meantime, the subsystem tests with the control computer and the development of the control system software were underway. The subsystem tests with beam were carried out whenever necessary. The storage ring commissioning started in April 1993 and we had beam stored very soon.

V. COMMISSIONING

A. Milestones

We began the BTS beam tests in August 1992 when the lower level section of the transfer line was completed. By September, the beam reached the septum entrance point. After the pulsed magnets had been installed, the beam passed through the septum and was injected into the ring in January 1993. In February 23, beam revolution, for the first time, was accomplished using one kicker for on-axis injection. Beam was observed in each screen monitor without using any corrector. It showed that many subsystems were basically in good condition. The beam sizes in the screen were consistent with the theoretical values and the alignment errors proved to be barely acceptable in the horizontal plane and extremely good in the vertical plane. Due to the long half-sine base width of 1.6 μs (400 ns revolution time) of the kicker pulse and there was only one kicker available at that time, the second turn observation was impossible. Soon after all the four kickers were available in April, we had several hundred beam revolutions using a few correctors without RF power and beam was captured on April 13, 1993 after turning on the RF power with minor adjustments of the magnet settings and RF frequency. The stored beam current was a few mA and beam lifetime was a few minutes under vacuum pressure of 10^{-7} Torr. A summary of the storage ring commissioning milestones is given in Table 3.

Table 3. Commissioning Milestones

Feb. 23, '93	First turn (on-axis injection at 1.3 GeV)
Apr. 2, '93	First few turns
Apr. 13, '93	First beam stored
Apr. 26, '93	Closed orbit measured using BPMs

B. Closed Orbit

We performed the closed orbit distortion measurements soon after the BPM system was working and the orbit distortion was corrected down to 0.5 mm and 0.3 mm rms in the horizontal and vertical plane, respectively, using the on-line application programs [10]. Further suppression of the orbit distortions will be obtained as the BPM offset and nonlinear calibration data are built into the database. The preliminary results of the closed orbit distortion measurements without using the corrector were fairly consistent with the simulation results using the existing alignment data and dipole field errors. Fig. 5 shows the closed orbit distortions before and after correction and the simulated results as well.

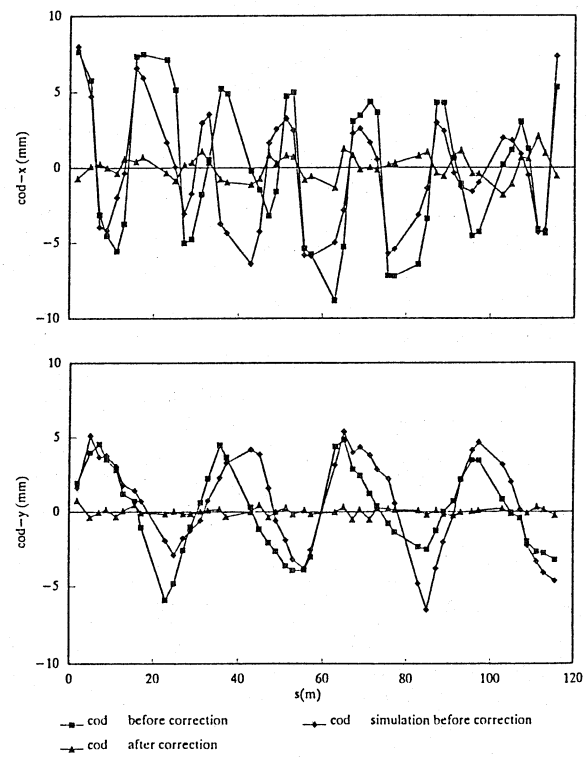

Fig. 5 Closed orbit distortions before and after correction in both transverse planes and the simulated orbit before correction.

C. Synchrotron Tune and Momentum Compaction Factor

The electron beam signal was picked-up with a stripline electrode and analyzed with a spectrum analyzer. The synchrotron sideband was measured and the momentum compaction factor was extracted. The measured momentum compaction factor was 0.00663 and was in good agreement with the design value of 0.00678.

D. Betatron Tune and Betatron Function

The turn-by-turn signal from one BPM electrode was FFT analyzed after the electron beam was kicked using one of the kicker magnet with about 1 mrad in the horizontal plane. The betatron sidebands were observed. The measured horizontal tune was ν_x = 7.142 at the nominal sextupole strengths under the corrected orbit. The vertical tune ν_y = 4.170 was obtained from the orbit changes with the vertical corrector setting. We will measure the transverse tunes using the tracking generator and spectrum analyzer system at the second commissioning stage. The optimum working point will be searched to get more beam storage current. By varying the quadrupole strength and measuring the horizontal tune shift, we obtained the averaged betatron function at each family of the quadrupole location. The result was in good agreement with the design value. From the orbit change when a vertical corrector was excited, the vertical betatron function was found to be in agreement with the design value [10].

E. Dispersion Function and Chromaticity

The dispersion function was deduced from the orbit difference with different RF frequency setting. In Fig. 6 the measured horizontal dispersion function as well as the designed value are shown. The vertical dispersion was very small. The horizontal chromaticity was measured by observing the tune shift with the RF frequency change. The horizontal chromaticity was corrected to about zero at the nominal sextupole strengths.

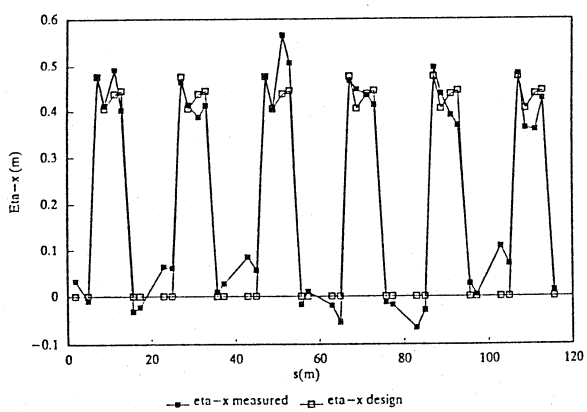

Fig. 6 The measured and designed dispersion function.

F. Beam Energy and Circumference

The injected beam energy was defined by varying the magnet setting and RF frequency. From the closed orbit distortions, one could obtain the energy deviation from the magnet settings. The injected beam energy could be measured to a precision of about 0.1%. From the survey and alignment data, the circumference deviated from the design value of 200 m was no more than 1 mm, which was consistent with the closed orbit data.

G. Bunch Length and Beam Size Measurement

The electron beam signal which was picked-up with the stripline electrode was analyzed with a fast digital sampling oscilloscope to obtain the bunch length as shown in Fig. 7. The measured bunch length σ_ℓ of 42 ps at 300 kV RF peak voltage was in good agreement with the theoretical value of 37 ps.

The transverse beam profile was measured from the synchrotron light out of the bending magnet with the XCC77RR high resolution CCD camera. The video signal was captured by a frame grabber and the transverse profile information was extracted. Fig. 8 displays the preliminary result.

VI. ACKNOWLEDGMENT

The authors would like to thank the entire SRRC staff involved in the design, construction and commissioning of such a delicate complex. Without their hardwork and full commitment, this early success would not have been possible. Thanks are also extended to outside advisers for their invaluable guidance, advice and suggestions.

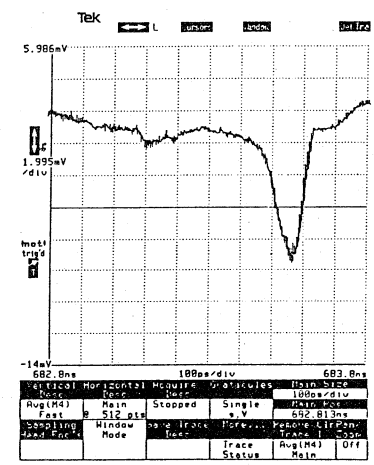

Fig. 7 The bunch length measured using the Tek11801A digital sampling oscilloscope. The signal was from the stripline electrode. The measured bunch length was about 100 ps in FWHM with 300 kV RF gap voltage.

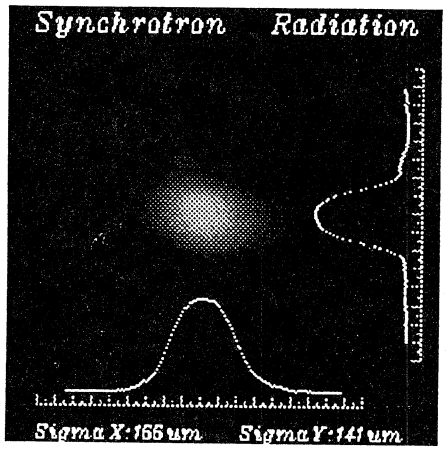

Fig. 8 Preliminary result of the synchrotron radiation profile measurement. Note that the depth of the field and the diffraction effect are not corrected.

VII. REFERENCES

[1] "SRRC Design Handbook", SRRC, 1991.

[2] K.K. Lin, K.T. Hsu and T.S. Ueng, "Measurement on the SRRC 1.3 GeV Electron Booster Synchrotron Operation Parameters and the Ramping Behaviour", PAC93, Washington D.C..

[3] M.H. Wang, C.C. Kuo and C.S. Hsue, "The Booster to Storage Ring Transport Line for SRRC", IEEE PAC91, Vol. 5, pp. 2697-2699.

[4] C.S. Hsue, C.C. Kuo, J.C. Lee and M.H. Wang, "Lattice Design of the SRRC 1.3 GeV Storage Ring", IEEE PAC91, Vol. 4, pp. 2670-2672.

[5] C.C. Kuo, C.S. Hsue, J.C. Lee, M.H. Wang and H.P. Chang, "Beam Dynamics of the SRRC 1.3 GeV Storage Ring", IEEE PAC91, Vol. 4, pp. 2667-2669.

[6] A. Wrulich, RACETRACK, DESY-84-07, 1984.

[7] C.H. Chang, H.C. Liu and G.J. Hwang, "Design and Performance of the Dipole Magnet for SRRC Storage Ring", PAC93, Washington D.C..

[8] G. Jan and K.T. Hsu, "Diagnostic Instrumentation System for the SRRC 1.3 GeV Synchrotron Radiation Light Source", PAC93, Washington D.C..

[9] J.S. Chen, C.J. Wang, S.J. Chen and G.J. Jan, "A Graphical User-Interface Control System at SRRC", PAC93, Washington D.C..

[10] P. Chang, C.H. Chang, C.C. Kuo, M.H. Wang, J.C. Lee, J.Y. Fan, H.J. Tasi and C.S. Hsue, "Machine Physics Application Program for Control, Commissioning and Error Findings for Storage Rings", PAC93, Washington D.C..